Traffic & Transportation

The Robust Two-Echelon Inventory Routing Problem for Vaccine Supply System – A Heuristic Method

Gang CHEN[1], Yunjian JIANG[2], Zhongyong CHEN[3], Bingshan MA[4], Luan SU[5]

Original Scientific Paper
Submitted: 4 June 2025
Accepted: 1 Sept 2025
Published: 28 Apr 2026

[1] Corresponding author, gc1991@chd.edu.cn, Zhejiang Scientific Research Institute of Transport, Hangzhou, China
[2] yjjiang1994@foxmail.com, Zhejiang Scientific Research Institute of Transport, Hangzhou, China
[3] med-zychen@foxmail.com, Information Centre, Zhejiang Drug Administration Bureau, Hangzhou, China
[4] bshanma1994@chd.edu.cn, Zhejiang Scientific Research Institute of Transport, Hangzhou, China
[5] luans1989@foxmail.com, Zhejiang Scientific Research Institute of Transport, Hangzhou, China

Publisher:
Faculty of Transport and Traffic Sciences, University of Zagreb

ABSTRACT
Vaccine supply chains confront several challenges in guaranteeing security of vaccines from the phase of production to the injection. Thus, it is crucial to construct a robust vaccine supply system that helps store and deliver vaccines safely and effectively. Inspired by a real-world vaccine supply case, this paper studies a robust two-echelon inventory routing problem that integrates the optimisation of vendor managed inventory (VMI), inventory policy and vehicle routing. A deterministic model is formulated to jointly optimise two-echelon vehicle routes as well as inventory at both distribution warehouse and vaccine demand nodes. Then, a robust modelling approach is introduced and converted into an equivalent linear form. An efficient solution algorithm is proposed, merging simulated annealing (SA) and adaptive large neighbourhood search (ALNS) to address large-scale cases. The computational efficiency of the proposed algorithm is demonstrated through numerical comparisons to the solutions founded by CPLEX and ALNS. The relation between input parameters and optimised results is investigated by a real-world vaccine supply system. The findings from results and sensitivity analyses suggest some interesting managerial implications.

KEYWORDS
vaccine supply chain; inventory-routing; two-echelon system; robust optimisation; heuristic method.

1. INTRODUCTION

Vaccines are considered as the first line to control and defend against infectious diseases all around the world [1]. Due to the limited shelf life and the specific customers of the vaccines, the stability of the vaccine supply chain (VSC) is of critical importance [2, 3]. The VSC is a strictly temperature-controlled cold chain system that must maintain a specific temperature range, which leads to high inventory and delivery costs [4, 5]. However, the locations of vaccine demand nodes (e.g. centres for disease control, hospitals, clinics and community health service) are widely scattered, and the vaccine demand for each node is uncertain [6]. Frequent deliveries from the vaccine supplier to the demand nodes are costly and time-consuming. Therefore, ensuring the cost-efficient and timely delivery for vaccines presents a significant challenge for the suppliers.

This study is inspired by a real-world case operated by a Chinese vaccine supplier. To reduce the delivery cost and enhance the time efficiency, the supplier has implemented a two-echelon (VMI) strategy in partnership with a cold chain pharmacy logistics company. In the first echelon, after lot release, vaccines are delivered from the supplier to the distribution warehouse near the demand nodes [7]. The vaccines stored in the distribution warehouse are still controlled by the supplier. In the second echelon, the logistics company performs regular replenishments from the distribution warehouse to the demand nodes. Each demand node

also has a small warehouse to temporarily store the vaccine. Additionally, the exact vaccine demand cannot be accurately predicted at each demand node in real-world situations, thus, the uncertain demand fluctuations of vaccine demand node should be considered as well.

Therefore, the study problem can be described as the combinatorial optimisation to simultaneously determine the two-echelon inventory strategy and route planning with the aim of minimised total cost and vaccine shortage considering the uncertain fluctuation of vaccine demand.

1.1 Literature review

As mentioned above, this study is related to the two-echelon inventory routing problem and the robust inventory optimisation. Thus, in this section, a comprehensive review from three streams of previous literature will be conducted: (1) two-echelon inventory routing problem (TEIRP); (2) inventory routing problem in the robust environment; (3) two-echelon inventory routing problem in the robust environment.

Two-echelon inventory routing problem (TEIRP). TEIRP is extended from the one-echelon inventory routing problem (IRP) proposed by Federgruen (1984) [8]. Different from IRP, TEIRP simultaneously optimises the inventory and vehicle routes for a two-echelon system. Some extensions of TEIRP were recently studied. Several studies focused on single-warehouse TEIRP where the two-echelon configuration contains the supplier, a distribution warehouse and a set of retailers. Jung et al. [9] firstly studied single-warehouse TEIRP and proposed an efficient heuristic procedure to break down the problem into three subproblems, namely retailer clustering, retailer sequencing and inventory policy. Zhao et al. [10] further provided a variable large neighbourhood search algorithm (VLNS) to optimise single-warehouse TEIRP. Li et al. [11] considered the direct delivery from the supplier to retailers in single-warehouse TEIRP and developed a decomposition solution approach. Nambirajan et al. [12] modelled a single-warehouse TEIRP considering multi-product and proposed a two-stage heuristic to solve the problem. Rohmer et al. [13] integrated customer delivery pattern in the single-warehouse TEIRP for perishable products and presented an adaptive large neighbourhood search (ALNS) based heuristic. Several studies focused on multi-warehouse TEIRP where the retailers can be assigned to different distribution warehouses. Nakhjirkan et al. [14] studied multi-warehouse TEIRP considering multi-product and developed a genetic algorithm (GA). Guimarães et al. [15] further proposed an ALNS-based heuristic to optimise the multi-warehouse TEIRP. Schenekemberg et al. [16] presented a multi-warehouse TEIRP with fleet management for petrochemical delivery and developed a branch-and-cut algorithm and an ALNS-based heuristic. Farias et al. [17] offered a two-step matheuristic combined with branch-and-cut algorithm to solve multi-warehouse TEIRP. Charaf et al. proposed a branch-and-cut algorithm with labelling algorithm [18] and tabu-search-based matheuristic [19] to solve multi-warehouse TEIRP. As discussed above, several previous studies have focused on TEIRP and the corresponding solution algorithm, while few studies consider uncertain customer demand in TEIRP and rare research is found concerning TEIRP in the vaccine supply system.

Inventory routing problem in the robust environment. Compared to deterministic environment, the robust environment is closer to the real world where some parameters may be uncertain. In order to solve the optimisation problem in the robust environment, Soyster (1973) [20] firstly proposed a robust approach to consider linear programming with the uncertain sets of parameters. Bertsimas et al. [21, 22] further developed a robustness approach allowing the parameters to deviate from their nominal value, where the level of conservatism can be controlled by a pre-specialised number. Then, the robustness approach was applied to different types of optimisation problems to control the uncertainty. As for IRP, Huang et al. [23] studied the IRP with stochastic stockout amount in vending machine supply chain and developed a modified ant colony algorithm (ACO). Solyalı et al. [24] combined the IRP with the robustness approach developed by Bertsimas et al. [22] and proposed a branch-and-cut algorithm. Soysal et al. [25] modelled an IRP with stochastic demand for fresh tomato supply chain and offered a simulation model algorithm to solve it. Li et al. [26] considered inventory inaccuracy caused by stock loss in IRP and designed a probability updating method. Jafarkhan et al. [27] formulated an IRP with supply and demand uncertainties for red blood cells supply chain and developed an ALNS-based heuristic. Fardi et al. [28] developed a cooperative IRP with the robustness approach developed by Bertsimas et al. [22] and employed ACO to solve the model. Rodrigues et al. [29] and Liu et al. [30] employed the robustness approach of Bertsimas et al. [22] and distributionally robust optimisation respectively and studied the IRP considering uncertain travel time for the maritime transportation. Taghipour et al. [31] employed the possibilistic optimisation method to study the inventory management for the vaccine supply chain while the vehicle routes are not optimised in the model. Li et al. [32] and Ortega et al. [33] studied the IRP considering scenario-based distributionally robust demands and dynamic demands, respectively. It can

be observed that a wide variety of studies have applied the robust approach to IRP, but the robust optimisation is rarely considered in TEIRP especially for the vaccine supply system.

Two-echelon inventory routing problem in the robust environment. To our best knowledge, only a few scholars studied robust-TEIRP-related problems. Ji et al. [34] introduced three uncertain sets (e.g. box, ellipsoid and polyhedron) into TEIRP and constructed a robust integer linear model for perishable products supply chain. However, vehicle routes and the inventory at customers were not optimised in the model. Shang et al. [35] and Rave et al. [36] both focused on healthcare supply chain and proposed a robust location routing problem (LIPR) and a TEIRP with stochastic demand respectively, while the inventory with customers and shortage of products are not considered in the models. Shiri et al. [37] proposed a two-stage approach to optimised vaccine supply chain, where the uncertainty of vaccine demand was estimated by machine learning, while the vehicle route optimisation was not included in the approach.

1.2 Contribution of the study

A summary of the relevant previous literature is listed in *Table 1*. Rare research on the robust TEIRP considering multi-products, products shortage and inventory at both distribution warehouse and customers is reported in the previous literature. Inspired by a real-world problem existed in vaccine supply system, a novel robust TEIRP model is proposed to optimise the two-echelon vaccine supply system with single distribution warehouse and provide a tangible heuristic to solve the problem. The principal contributions of this research include:

1) To minimise inventory costs, delivery costs and vaccine shortage cost, a novel mixed integer linear TEIRP is proposed to simultaneously optimise two-echelon vehicle routes as well as inventory at both distribution warehouse and vaccine demand nodes.
2) A robust modelling approach is employed to address the uncertain vaccine demand in TEIRP, and its equivalent linear form is yielded by introducing dual variables.
3) A tangible solution algorithm combining SA and ALNS is proposed to solve the large-scale robust TEIRP efficiently.
4) The results and sensitivity analyses based on the developed robust TEIRP and real-world case study provide some interesting insights, which would help decision-makers assess the performance of the two-echelon vaccine supply system.

Table 1 – Summary of the previous TEIRP literature

Reference	Robust/ Deterministic	Solution algorithm	Single/Multiple distribution warehouse	Inventory		Multiple products	Products shortage
				At distribution warehouse	With customers		
Jung et al. [9]	Deterministic	Heuristic	Single	✓	✓		
Zhao et al. [10]	Deterministic	Heuristic	Single	✓	✓		
Li et al. [11]	Deterministic	Heuristic	Single	✓	✓		
Nambirajan et al. [12]	Deterministic	Heuristic	Single	✓	✓	✓	
Rohmer et al. [13]	Deterministic	Heuristic	Single	✓		✓	
Nakhjirkan et al. [14]	Deterministic	Heuristic	Multiple	✓		✓	✓
Guimarães et al. [15]	Deterministic	Heuristic	Multiple	✓	✓		
Schenekemberg et al. [16]	Deterministic	Exact	Multiple	✓	✓		
Farias et al. [17]	Deterministic	Exact	Multiple	✓	✓		
Charaf et al. [18]	Deterministic	Exact	Multiple	✓	✓		
Charaf et al. [19]	Deterministic	Heuristic	Multiple	✓	✓		
Ji et al. [34]	Robust		Multiple	✓			
Shang et al. [35]	Robust		Multiple	✓		✓	
Rave et al. [36]	Robust	Heuristic	Single	✓		✓	
This study	Robust	Heuristic	Single	✓	✓	✓	✓

The remainder of this paper is organised as follows: Section 2 introduces the background information and formulates deterministic and robust TEIRPs for the vaccine supply system. The solution algorithm and corresponding computational results are detailed in Section 3. A real-world case study is investigated in Section 4, where the optimal results and sensitivity analyses are discussed. Section 5 presents some concluding remarks and outlines potential future directions.

2. PROBLEM DESCRIPTION AND FORMULATION

Similar to single-warehouse TEIRP, the study vaccine supply system is two-echelon, which contains a vaccine supplier, a distribution warehouse and several vaccine demand nodes. The vaccine supplier produces different types of vaccines for the vaccine demand nodes. The distribution warehouse, which belongs to the third-party logistics service, receives vaccines from the supplier and then stores them until delivery occurs. Each demand node (e.g. hospitals, clinics and community healthcare service) owns a small warehouse, which can temporarily store small amounts of vaccines as needed.

Time in the study vaccine supply system is separated into a set of discrete fixed-time periods. In each period, the logistics company delivers vaccines to the distribution warehouse and demand nodes separately, and the vaccine amount delivered to them is determined by the inventory level at the end of the preceding period. The warehouse inventory level is updated at the end of each period.

The vehicles used in the study vaccine supply system are divided into two types. The first type is first-echelon vehicle with larger capacity, which is applied in the long-distance delivery from the vaccine supplier to the distribution warehouse. The second type is second-echelon vehicle with smaller capacity, which is applied in the short-distance delivery from the distribution warehouse to the vaccine demand nodes.

Figure 1 illustrates a sample two-echelon vaccine supply network containing one supplier, one distribution warehouse, six demand nodes and two periods. In the first period, two second-echelon vehicles are employed to serve all six demand nodes. Thus, two routes (0-1-2-0 and 0-3-4-5-6-0) are formed. In the second period, four demand nodes are served by one second-echelon vehicle and the route is 0-2-4-5-6-0.

Therefore, the study problem is to simultaneously determine optimal delivery schedule and vehicle routes from distribution warehouse to demand nodes and optimise the amount of vaccine stored at both distribution warehouse and demand nodes, minimising two-echelon delivery and inventory costs, while taking the vaccine shortage penalty cost into account in each period.

Subsequently, model assumptions and mathematical notations are presented, followed by the formulation of corresponding models considering both deterministic and uncertain vaccine demands.

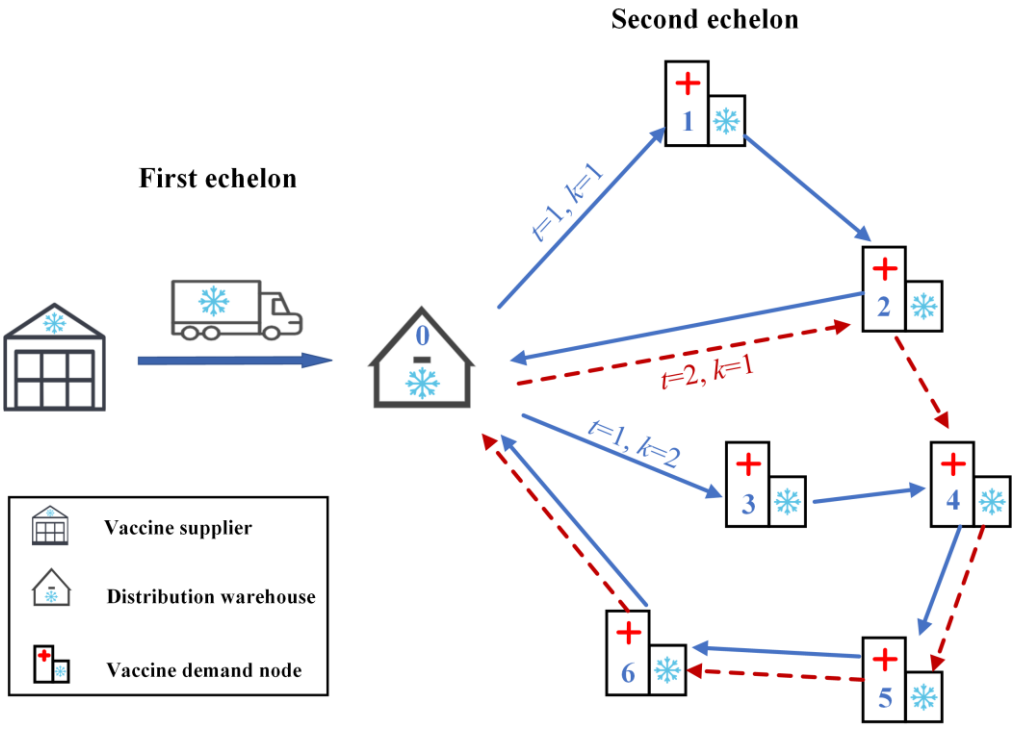

Figure 1 – Sample two-echelon vaccine delivery network

2.1 Problem assumption

Several assumptions are stated before presenting the model formulations.

1) The locations of the supplier, distribution warehouse and vaccine demand nodes are fixed and given.
2) The nominal vaccine demands of vaccine demand nodes can be obtained from historical data.
3) In each period, first-echelon vehicle can travel multiple times between the vaccine supplier and the vaccine distribution warehouse.
4) In each period, each vaccine demand node can be served at most once by one second-echelon vehicle.
5) Each second-echelon vehicle starts and ends at the vaccine distribution warehouse.

2.2 Notations

The mathematical notations used in the model formulation are defined as follows:

Sets

N, set of nodes including distribution warehouse indexed by i, j {distribution warehouse: 0; vaccine demand nodes: 1, …, N };

K, set of second-echelon vehicles for delivering vaccine from distribution warehouse to vaccine demand nodes indexed by k, $k \in \{1,...,K\}$;

T, set of time periods indexed by t, t', $t,t' \in \{1,...,T\}$;

M, set of vaccine types indexed by m, $m \in \{1,...,M\}$.

Parameters

r_{ij} , routing cost from node i to node j;

t_{ij}, travel time from node i to node j;

C, first-echelon routing cost between supplier and distribution warehouse;

Q , capacity of the first-echelon vehicle;

q , capacity of the second-echelon vehicle;

T, maximum travel time allowed for the second-echelon vehicle;

IW , inventory holding capacity of distribution warehouse;

IS_i , inventory holding capacity of vaccine demand nodes;

d_{im}^t , demand of vaccine m in vaccine demand node i in time period t;

W , unit vaccine holding cost in distribution warehouse;

w , unit vaccine holding cost in vaccine demand nodes;

iw_m^0 , initial inventory level of vaccine m in distribution warehouse;

is_{im}^0 , initial inventory level of vaccine m in vaccine demand node i;

v_m , unit volume of vaccine m;

l , unit shortage penalty cost of vaccine m in vaccine demand nodes.

Variables

x_{ij}^{tk} , 1 if vehicle k travels from node i to j in time period t, otherwise 0;

y_i^{kt} , 1 if vehicle k visits vaccine demand node i in time period t, otherwise 0;

a_{im}^{tk}, quantities of vaccine m delivered from distribution warehouse to vaccine demand node i by vehicle k in time period t;

b_m^t , quantities of vaccine m delivered from supplier to distribution warehouse in time period t;

n^t , number of vehicles used from supplier to distribution warehouse in time period t;

iw^t , inventory level of distribution warehouse at the end of time period t;

is_i^t , inventory level of vaccine demand node i at the end of time period t;

u_i^{tk} , auxiliary variable to eliminate subtour.

2.3 Deterministic model

As shown in *Equation 1*, the objective function consists of four parts. The first part is the linehaul delivery cost from the supplier to the distribution warehouse in the first echelon. The second part is the delivery cost from the distribution warehouse to vaccine demand nodes in the second echelon. The third part is the inventory cost in the distribution warehouse. The fourth part is the cost incurred in the vaccine demand node. If the inventory level of vaccine demand node is greater than 0, the inventory cost will be incurred. Otherwise, the vaccine shortage cost will be incurred.

$$\min Z = \sum_{t\in T} Cn^t + \sum_{t\in T}\sum_{k\in K}\sum_{i\in N}\sum_{j\in N} r_{ij}^k x_{ij}^{kt} + W\sum_{t\in T}\sum_{m\in M} v_m iw_m^t + \sum_{t\in T}\sum_{m\in M}\sum_{i\in N} \max\left(is_{im}^t w, -is_{im}^t l \right) \tag{1}$$

st:

$$iw_m^t = iw_m^{t-1} + b_m^t - \sum_{i\in N\setminus\{0\}}\sum_{k\in K} a_{im}^{tk} \qquad \forall t\in T, m\in M \tag{2}$$

$$\sum_{m\in M} v_m iw_m^t \le IW \qquad \forall t\in T \tag{3}$$

$$iw_m^t \ge 0 \qquad \forall t\in T, m\in M \tag{4}$$

$$\sum_{m\in M} v_m b_m^t \le Q\, n^t \qquad \forall t\in T \tag{5}$$

$$is_{im}^t = is_{im}^{t-1} - d_{im}^t + \sum_{k\in K} a_{im}^{tk} \qquad \forall i\in N\setminus\{0\}, t\in T, m\in M \tag{6}$$

$$\sum_{m\in M} v_m is_{im}^t \le IS_i \qquad \forall i\in N\setminus\{0\}, t\in T \tag{7}$$

$$\sum_{i\in N\setminus\{0\}}\sum_{m\in M} v_m a_{im}^{tk} \le \sum_{i\in N\setminus\{0\}} q y_i^{kt} \qquad \forall k\in K,\ t\in T \tag{8}$$

$$\sum_{k\in K} y_i^{kt} \le 1 \qquad \forall i\in N\setminus\{0\}, t\in T \tag{9}$$

$$y_i^{kt} \le \sum_{j\in N} x_{ij}^{tk} \qquad \forall i\in N\setminus\{0\}, t\in T \tag{10}$$

$$\sum_{i\in N} x_{i0}^{tk} = \sum_{j\in N} x_{0j}^{tk} \qquad \forall k\in K, \forall t\in T \tag{11}$$

$$\sum_{j\in N} x_{ij}^{tk} = \sum_{j\in N} x_{ji}^{tk} \qquad \forall k\in K, \forall t\in T \tag{12}$$

$$u_i^{tk} - u_j^{tk} + N x_{ij}^{tk} \le N-1 \qquad \forall i,j\in N\setminus\{0\}, k\in K, t\in T \tag{13}$$

$$\sum_{i\in N}\sum_{j\in N} t_{ij} x_{ij}^{tk} \le T \qquad \forall k\in K, \forall t\in T \tag{14}$$

$$x_{ij}^{tk}, y_j^{tk} \in \{0,1\} \tag{15}$$

$$a_{im}^{tk}, b_m^t, u_i^{tk} \ge 0 \tag{16}$$

$$n^t \in \mathbb{Z} \tag{17}$$

Equations 2–5 are constraints for the first echelon. *Equation 2* links the inventory level of distribution warehouse in periods *t* and *t-1*. *Equations 3–4* guarantee that the inventory level of distribution warehouse cannot be negative while not exceeding the inventory holding capacity. *Equation 5* imposes a vehicle capacity for first-echelon delivery.

Equations 6–14 are constraints for the second echelon. *Equation 6* links the inventory level of demand nodes in periods *t* and *t-1*. *Equation 7* guarantees that the inventory level of demand nodes cannot exceed the inventory holding capacity. *Equation 8* imposes a vehicle capacity for second-echelon delivery. *Equations 9–13* are second-

echelon vehicle routing constraints. *Equation 9* restricts that each demand node can be served at most once in each period. *Equation 10* ensures that a delivery from the distribution warehouse to a demand node can only be made by an activated second-echelon vehicle. *Equation 11* states that each second-echelon vehicle starts and terminates at distribution warehouse. *Equation 12* is the second-echelon vehicle flow equilibrium constraint. *Equation 13* is used to eliminate the subtour of second-echelon vehicle routes. *Equation 14* enforces that the second-echelon delivery is within travel time limit.

The feasible domains of the decision variables are defined by *Equations 15–17*.

To further simplify the model, *Equations 2, 6* are replaced by *Equations 18, 19*.

$$iw_m^t = iw_m^0 + \sum_{t'=1}^{t}(b_m^{t'} - \sum_{i\in N\setminus\{0\}}\sum_{k\in K} a_{im}^{t'k}) \quad \forall t\in T, m\in M \tag{18}$$

$$is_{im}^t = is_{im}^0 + \sum_{t'=1}^{t}(\sum_{k\in K} a_{im}^{t'k} - d_{im}^{t'}) \quad \forall i\in N\setminus\{0\}, t\in T, m\in M \tag{19}$$

Hence, the deterministic model can be modelled as follows:

$$\begin{aligned}\min Z = &\sum_{t\in T}\sum_{k\in K}\sum_{i\in N}\sum_{j\in N} c_{ij}^k x_{ij}^{kt} + \sum_{t\in T} Cn^t + W\sum_{t\in T}\sum_{m\in M} v_m\left[iw_m^0 + \sum_{t'=1}^{t}(b_m^{t'} - \sum_{i\in N\setminus\{0\}}\sum_{k\in K} a_{im}^{t'k})\right] \\ &+ \sum_{t\in T}\sum_{m\in M}\sum_{i\in N}\max\left[w\left(is_{im}^0 + \sum_{t'=1}^{t}\sum_{k\in K} a_{im}^{t'k} - \sum_{t'=1}^{t} d_{im}^{t'}\right), l\left(\sum_{t'=1}^{t} d_{im}^{t'} - is_{im}^0 - \sum_{t'=1}^{t}\sum_{k\in K} a_{im}^{t'k}\right)\right]\end{aligned} \tag{20}$$

st:

Equations 5, 8–17,

$$\sum_{m\in M} v_m\left[iw_m^0 + \sum_{t'=1}^{t}(b_m^{t'} - \sum_{i\in N\setminus\{0\}}\sum_{k\in K} a_{im}^{t'k})\right] \le IW \quad \forall t\in T \tag{21}$$

$$iw_m^0 + \sum_{t'=1}^{t} b_m^{t'} \ge \sum_{t'=1}^{t}\sum_{i\in N\setminus\{0\}}\sum_{k\in K} a_{im}^{t'k} \quad \forall t\in T, m\in M \tag{22}$$

$$\sum_{m\in M} v_m\left[is_{im}^0 + \sum_{t'=1}^{t}(\sum_{k\in K} a_{im}^{t'k} - d_{im}^{t'})\right] \le IS_i \quad \forall i\in N\setminus\{0\}, t\in T \tag{23}$$

2.4 Robust model

In realistic cases, the vaccine demand of each demand node may deviate from its expected value. The uncertainty in vaccine demand deviation may incur extra vaccine inventory cost or vaccine shortage. Based on the observation from the historical data, the deviations are not entirely random or unlimited. The range of demand deviation based on historical trends can be estimated, including the nominal value and the maximum deviation of the vaccine demand.

To address the vaccine demand uncertainty, a robust optimisation approach provided by Bertsimas et al. (2004) [22] is implemented to control the degree of conservatism. A vaccine demand uncertainty set U_{im}^t in *Equation 24* is estimated. It can be seen that each vaccine demand d_{im}^t is assumed to be an independent random variable in the uncertainty set U_{im}^t. d_{im}^t can be calculated by $d_{im}^t = \bar{d}_{im}^t + \Delta_{im}^t \hat{d}_{im}^t$, where $\bar{d}_{im}^t$ is the nominal value of the vaccine demand, Δ_{im}^t is the random deviation coefficient of vaccine demand deviation, $\hat{d}_{im}^t$ is the maximum demand deviation estimated from historical data. $\left|\Delta_{im}^t\right| \le 1$ restricts that the vaccine demand deviation in each time period cannot exceed the maximum demand deviation, meaning that d_{im}^t can only take value from the range $[\bar{d}_{im}^t - \hat{d}_{im}^t, \bar{d}_{im}^t + \hat{d}_{im}^t]$.

Additionally, a parameter Γ_{im}^t is introduced, which is the degree of conservatism during *t* time periods for the vaccine demand *m* at node *i*. Γ_{im}^t is an input parameter determined by decision-makers. Larger Γ_{im}^t means higher degree of conservatism, indicating that decision-makers perceive a larger deviation of vaccine demand

during t time periods. Γ^t_{im} can be calculated by $\Gamma^t_{im} = \beta_{im} t$, where β_{im} ($0 \le \beta_{im} \le 1$) is an input coefficient estimated by decision-makers, meaning the degree of conservatism of vaccine demand m at demand node i in each time period. Specifically, if $\beta_{im} = 0$, $\Gamma^t_{im} = 0$, which means there is no protection against uncertainty, and the model turns to be deterministic. Thus, in *Equation 24*, $\sum_{h=1}^{t} \left|\Delta^h_{im}\right| \le \Gamma^t_{im}$ means that the vaccine demand deviation during t time periods cannot exceed maximum demand deviation estimated by decision-makers.

$$U^t_{im} = \left\{ d^t_{im} : d^t_{im} = \bar{d}^t_{im} + \Delta^t_{im} \hat{d}^t_{im}, \left|\Delta^t_{im}\right| \le 1, \sum_{h=1}^{t} \left|\Delta^h_{im}\right| \le \Gamma^t_{im} \right\}, \forall i \in N, m \in M, t \in T \tag{24}$$

Hence, the robust model can be modelled as follows:

$$\begin{aligned} \min Z = {} & \sum_{t\in T}\sum_{k\in K}\sum_{i\in N}\sum_{j\in N} c^k_{ij} x^{kt}_{ij} + \sum_{t\in T} Cn^t + W \sum_{t\in T}\sum_{m\in M} v_m \left[iw^0_m + \sum_{t'=1}^{t} (b^{t'}_m - \sum_{i\in N\setminus\{0\}}\sum_{k\in K} a^{t'k}_{im}) \right] \\ & + \sum_{t\in T}\sum_{m\in M}\sum_{i\in N} \max\left[w\left(is^0_{im} + \sum_{t'=1}^{t}\sum_{k\in K} a^{t'k}_{im} - \min_{d^t_{im}\in U^t_{im}} \sum_{t'=1}^{t} d^{t'}_{im} \right), l\left(\max_{d^t_{im}\in U^t_{im}} \sum_{t'=1}^{t} d^{t'}_{im} - is^0_{im} - \sum_{t'=1}^{t}\sum_{k\in K} a^{t'k}_{im} \right) \right] \end{aligned} \tag{25}$$

st:

Equations 5, 8–17, 21–23,

$$\sum_{m\in M} v_m \left(is^0_{im} + \sum_{t'=1}^{t}\sum_{k\in K} a^{t'k}_{im} - \min_{d^t_{im}\in U^t_{im}} \sum_{t'=1}^{t} d^{t'}_{im} \right) \le IS_i \qquad \forall i \in N\setminus\{0\}, t \in T \tag{26}$$

The proposed robust model is a non-linear formulation due to *Equations 25, 26*. To obtain linear formulation, dual variables η^t_{im}, $\theta^{t't}_{im}$ and an auxiliary variable λ^t_{im} are introduced to transform the model into its equivalent linear formulation, which is given as follows:

$$\min Z = \sum_{t\in T}\sum_{k\in K}\sum_{i\in N}\sum_{j\in N} c^k_{ij} x^{kt}_{ij} + \sum_{t\in T} Cn^t + W \sum_{t\in T}\sum_{m\in M} v_m \left[iw^0_m + \sum_{t'=1}^{t} (b^{t'}_m - \sum_{i\in N\setminus\{0\}}\sum_{k\in K} a^{t'k}_{im}) \right] + \sum_{i\in N}\sum_{m\in M}\sum_{t\in T} \lambda^t_{im} \tag{27}$$

st:

Equations 5, 8–17, 21–23,

$$\lambda^t_{im} \ge l\left(\sum_{t'=1}^{t} \bar{d}^{t'}_{im} + \eta^t_{im}\Gamma^t_{im} + \sum_{t'=1}^{t} \theta^{t't}_{im} - is^0_{im} - \sum_{t'=1}^{t}\sum_{k\in K} a^{t'k}_{im} \right) \qquad \forall i \in N\setminus\{0\}, m \in M, t \in T \tag{28}$$

$$\lambda^t_{im} \ge w\left(is^0_{im} + \sum_{t'=1}^{t}\sum_{k\in K} a^{t'k}_{im} - \sum_{t'=1}^{t} \bar{d}^{t'}_{im} + \eta^t_{im}\Gamma^t_{im} + \sum_{t'=1}^{t} \theta^{t't}_{im} \right) \qquad \forall i \in N\setminus\{0\}, m \in M, t \in T \tag{29}$$

$$\sum_{m\in M} v_m \left(is^0_{im} + \sum_{t'=1}^{t}\sum_{k\in K} a^{t'k}_{im} - \sum_{t'=1}^{t} \bar{d}^{t'}_{im} + \eta^t_{im}\Gamma^t_{im} + \sum_{t'=1}^{t} \theta^{t't}_{im} \right) \le IS_i \qquad \forall i \in N\setminus\{0\}, t \in T \tag{30}$$

$$\eta^t_{im} + \theta^{t't}_{im} \ge \hat{d}^t_{im} \qquad \forall i \in N\setminus\{0\}, m \in M, t \in T \tag{31}$$

$$\eta^t_{im}, \theta^{t't}_{im}, \lambda^t_{im} \ge 0 \tag{32}$$

3. SOLUTION ALGORITHM

As discussed earlier, the proposed model incorporates two-echelon inventory management and vehicle routing problem (VRP), which has been proven to be NP-hard in several existing research [38, 39]. Optimal solutions of the problem can only be obtained for small-scale instances. As the scale of instances increases, the difficulty of obtaining the optimal solution grows exponentially. In order to find the solution efficiently, a heuristic algorithm based on simulated annealing (SA) and adaptive large neighbourhood search (ALNS)

framework structure are developed, where SA is utilised to diversify the searching process, and ALNS is employed to optimise the vehicle routes. Several previous research have proven that ALNS shows good performance in solving VRP-related problem due to its generality and flexibility [40, 41]. A TE-NFP (two-echelon network flow problem) model is proposed to effectively deal with the inventory optimisation. The detailed process of the proposed heuristic is discussed next.

3.1 Initialisation

In order to accelerate and improve the performance of the proposed solution algorithm, a cheapest-insertion-based heuristic is developed to generate a series of high-quality initial solutions within computationally acceptable timeframes. As described in *Algorithm 1*, the construction heuristic for initial solution is divided into two phases.

The first phase is to generate the vehicle routes in each period. 70%–85% of total vaccine demand nodes are randomly selected and then sequentially inserted into their optimal positions in the period route by the greedy insertion method. Then, the routes are optimised by the 2-opt procedure.

The second phase is to determine the other variables. A TE-NFP model is proposed to simultaneously optimise vaccine quantities delivered to distribution warehouse and demand nodes, inventory at distribution warehouse and demand nodes, quantities of vaccine shortage. CPLEX solver is employed to solve the TE-NFP. Note that TE-NFP is the reduced version of the proposed robust model provided in Section 2, where the visited demand nodes and vehicle routes in each period are generated and optimised in the first phase. Thus, decision variables x_{ij}^{tk} and y_i^{kt} are switched into input parameters in TE-NFP. The proposed TE-NFP is detailed as follows:

$$\min Z = \sum_{t\in T}\sum_{k\in K}\sum_{i\in N}\sum_{j\in N} c_{ij}^{k} x_{ij}^{kt} + \sum_{t\in T} Cn^{t} + W\sum_{t\in T}\sum_{m\in M} v_m \left[iw_m^0 + \sum_{t'=1}^{t}\left(b_m^{t'} - \sum_{i\in N\setminus\{0\}}\sum_{k\in K} a_{im}^{t'k}\right)\right] + \sum_{i\in N}\sum_{m\in M}\sum_{t\in T}\lambda_{im}^{t} \tag{33}$$

st:

Equations 5, 8–17, 21–23,28–32.

Algorithm 1 – Construction heuristic for initial solution

1. Initialise solution by setting time period t :=1.
2. **For** ($t \le T$) **do**
3. M :=Randomly select 70%–85% of all vaccine demand nodes;
4. Set vaccine demand node i :=0, route i :=1;
5. **For** ($i \le M$) **do**
6. Insert vaccine demand node i into its best insertion position in route r.
7. **If** (no feasible insertion positions are found) **then**
8. Create a new route and insert vaccine demand node i in the new route.
9. **End for**
10. **While** (the routing cost can be improved) **do**
11. 2-opt is applied to improving the route.
12. **End while**
13. **End for**
14. Solve the TE-NFP for vaccine quantities delivered to distribution warehouse and vaccine demand nodes, inventory at distribution warehouse and demand nodes, quantities of shortage.
15. **Return** initial feasible solution $S_{initial}$.

3.2 Main algorithm

Algorithm 2 details the general framework for the proposed heuristic. Simulated annealing is introduced to prevent the proposed heuristic from trapping in the local optima [42]. The inputs are the initial feasible solutions $S_{initial}$ provided by *Algorithm 1*, while the output is the optimised solutions S_{best} .

At first, a set of parameters (d, r, $iter$, w_d^{iter}, w_p^{iter}, t_s) are preset. Destroy operators and repair operators are selected from the lists based on their weights and applied to $S_{current}$ sequentially to obtain S_{repair}. The TE-NFP of S_{repair} is solved by CPLEX solver to obtain $Z(S_{repair})$. If $Z(S_{repair})$ improves on $Z(S_{current})$, S_{repair} is

accepted. Note that simulated annealing is introduced to diversify the searching process and prevent from trapping into cycling search. Following the Metropolis criterion, the inferior solutions are accepted with the predefined probability $\exp(\frac{-(Z(S_{repair})-Z(S_{current}))}{t}) \geq a$. The probability is decreased as the number of iterations increases. If $Z(S_{current})$ is better than $Z(S_{best})$, $S_{current}$ becomes the new best solution. The process is repeated until the terminating condition (e.g. max number of iteration) is met. The main components (e.g. destroy and repair operators, adaptive weight adjustment) of the general framework for the proposed heuristic are discussed next.

Algorithm 2 – General framework for the proposed heuristic

1. **Input:** Initial feasible solutions $S_{initial}$.
2. **Output:** Optimised solutions S_{best}.
3. Set number of iterations $iter$=1, 2..., $iter_{\max}$.
4. Set destroy operator $d \in D$ and repair operator $r \in R$.
5. Set weights of destroy operator w_d^{iter} and repair operator w_p^{iter}.
6. Set starting temperatures t_s.
7. $S_{best} \leftarrow S_{current} \leftarrow S_{initial}$
8. **While** $iter \leq iter_{\max}$ **do**
9. $t \leftarrow$ temperature $\frac{iter_{\max} - iter}{iter} t_s$.
10. Select a destroy operator *d* by roulette-wheel based on weights P_d.
11. Apply the selected destroy operator *d* to $S_{current}$ to obtain $S_{destroy}$.
12. Select a repair operator *r* by roulette-wheel based on weights P_r.
13. Apply the selected repair operator *r* to $S_{destroy}$ to obtain S_{repair}.
14. Solve the TE-NFP of S_{repair} for vaccine quantities delivered to distribution warehouse and customers, inventory at distribution warehouse and customers, quantities of vaccine shortage.
15. Calculate the total cost of S_{repair} to obtain $Z(S_{repair})$.
16. **If** $Z(S_{repair}) \leq Z(S_{current})$ **then**
17. $S_{current} \leftarrow S_{repair}$
18. **Else**
19. Randomly generate a number $a \in (0,1)$.
20. **If** $\exp(\frac{-(Z(S_{repair})-Z(S_{current}))}{t}) \geq a$ **then**
21. $S_{current} \leftarrow S_{repair}$
22. **End if**
23. **End if**
24. **If** $Z(S_{current}) \leq Z(S_{best})$ **then**
25. $S_{best} \leftarrow S_{current}$
26. **End if**
27. Update w_d^{iter} and w_p^{iter}.
28. $iter \leftarrow iter + 1$
29. **End while**
30. **Return** S_{best}

Destroy operators: Inspired by Coelho et al. [43] and Jafarkhan et al. [27], four specialised destroy operators that work at vaccine demand nodes and vehicle routes are developed by selectively removing a number of demand nodes from the current solution.

1) Random vaccine demand node removal
   One time period is stochastically chosen, and one demand node is randomly removed from it. This process is repeated α times.

2) Route-based vaccine demand node removal
One time period is stochastically chosen and β adjacent demand nodes in the same route are randomly removed.
3) Distance-based vaccine demand node removal
One period and one demand node from it are randomly selected. Then, all the demand nodes within *x* distance to the selected demand node in the same route are removed.
4) Cost-based vaccine demand node removal
One time period is stochastically chosen. Then, the demand node with the largest cost-saving potentials is removed from it. This process is repeated α times.

Repair operator: Some vaccine demand nodes removed in destruction process need to be reinserted in case that the solutions are severely destroyed. Thus, 3 repair operators are proposed as follows.

1) Random vaccine demand node insertion
One time period is stochastically chosen, and one unserved vaccine demand node is inserted to its best position considering total cost. This process is repeated α times.
2) Distance-based vaccine demand node insertion
One period and one unserved vaccine demand node in it are randomly selected. Then, the selected demand node and all the unserved demand nodes within *x* distance to it are inserted to its best position considering total cost.
3) Cost-based vaccine demand node insertion
One time period is stochastically chosen. The unserved vaccine demand node with the cheapest insertion cost is inserted in it. This process is repeated α times.

Adaptive weight adjustment mechanism: Adaptive weight adjustment mechanism is introduced to dynamically update the weights of destroy and repair operators in roulette wheel at each iteration [44]. The weights are calculated by evaluating their performance at the preceding iterations. Initially, each operator is assigned a weight and a score. The weights of 4 destroy operators and 3 repair operators are equally set as 1/4 and 1/3, respectively. In each iteration, the scores are updated as follows: if an operator identifies a new best solution, its score is incremented by σ_1; if it identifies a solution that is superior to the current solution, its score is increased by σ_2; if the solution does not outperform the current solution but is still accepted by the simulated annealing criterion, the score is augmented by σ_3. According to previous study, the scores σ_1, σ_2, σ_3 are set as 20, 10, 5, respectively. Thus, the updated weights are computed in *Equations 34–35*.

$$w_d^{iter+1} = w_d^{iter}(1-\varsigma) + \varsigma s_d / o_d \tag{34}$$

$$w_p^{iter+1} = w_p^{iter}(1-\varsigma) + \varsigma s_p / o_p \tag{35}$$

where w_d^{iter} and w_p^{iter} are weights of destroy and repair operators, respectively. $\varsigma \in (0, 1)$ is roulette-wheel reaction factor, determining the rate at which the weight adjustment responds to variations in the operator performance. s_d and s_p are scores of destroy and repair operators, respectively. o_d and o_p are the number of times that destroy and repair operators have been used at the preceding iterations, respectively.

3.3 Algorithm performance analysis

To evaluate the performance of the proposed heuristic (TPH), a set of instances based on real cases are generated based on the dataset provided by Rohmer et al. [13], which are available at https://tinyurl.com/25nya4yt. The instances are divided into three sets according to their time periods (T=2, 4, 6). In each set, the number of demand nodes ranges from 5 to 100 (n=5, 10, 15, 25, 50, 100). Other input parameters are generated from the real-world cases and listed in each instance. CPLEX, ALNS and TPH are employed to solve the instances. ALNS and TPH are implemented in MATLAB (version 2018a) and executed on an Intel Core i5 laptop (2.42 GHz, 16GB RAM), where CPLEX is linked to MATLAB for solving the TE-NFP. With the computational time limit of 2h (7200s), we conduct 20 runs for each instance and report the average results in *Table 1*, where the average optimised results of CPLEX, ALNS and TPH are denoted as Z_{CPLEX}, Z_{ALNS}, and Z_{TPH} respectively. The gaps between different optimised results (e.g. GAP_{AL-C}, GAP_{TPH-C}, GAP_{TPH-AL}) are calculated by *Equations 36–38.* Some computational parameters are adjusted according to instance size during the numerical experiments to obtain the optimised solutions.

$$GAP_{AL-C} = \frac{Z_{ALNS} - Z_{CPLEX}}{Z_{CPLEX}} * 100\% \quad (36)$$

$$GAP_{TPH-C} = \frac{Z_{TPH} - Z_{CPLEX}}{Z_{CPLEX}} * 100\% \quad (37)$$

$$GAP_{TPH-AL} = \frac{Z_{TPH} - Z_{ALNS}}{Z_{ALNS}} * 100\% \quad (38)$$

As is shown in the column headings of *Table 2*, the instances are classified into three sets according to the number of time periods. In each set, the number of demand nodes increases from 5 to 100. It can be found that for the small-scale instances ($n \leq 15$), CPLEX, ALNS and TPH can all obtain optimal solutions. As the number of demand nodes increases, CPLEX exhibits considerable growth in computational time, whereas ALNS and TPH demonstrate significantly superior computational efficiency in comparison. When the number of demand nodes reaches 25, the only feasible solutions can be found within the time limitation (7200s) for all three sets. As the instance size keeps increasing, CPLEX becomes computationally intractable and cannot return feasible solutions. Notably, compared to ALNS, TPH shows superior computational performance when solving larger-scale instances ($n \geq 50$). For the large instances ($t \geq 4,\ n \geq 50$), the optimised results obtained by TPH are on average 10.93% better than those obtained by ALNS.

Table 2 – Optimised results of different instances solved by CPLEX, ALNS and TPH

Number of time period	Number of demand nodes	CPLEX		ALNS			The proposed heuristic (TPH)			
		Z_{CPLEX}	Time (s)	Z_{ALNS}	GAP_{AL-C} (%)	Time (s)	Z_{TPH}	GAP_{TPH-C} (%)	GAP_{TPH-AL} (%)	Time (s)
T=2	n=5	1112.5	206.1	1112.5	0	37.3	1112.5	0	0	49.7
	n=10	1821.7	812.3	1821.7	0	50.6	1821.7	0	0	53.2
	n=15	2125.4	2485.3	2125.4	0	100.2	2125.4	0	0	98.4
	n=25	4286.1	7200[a]	3315.1	-22.65	345.6	3315.1	-22.65	0	362.5
	n=50	-	-	4856.6	-	687.5	4856.6	-	0	653.6
	n=100	-	-	7237.1	-	1356.2	6854.2	-	-5.29	1475.1
T=4	n=5	1645.2	254.3	1645.2	0	62.4	1645.2	0	0	84.2
	n=10	2412.4	1120.4	2412.4	0	87.5	2412.4	0	0	97.1
	n=15	2873.1	2781.1	2873.1	0	134.2	2873.1	0	0	152.4
	n=25	6875.3	7200[a]	5345.2	-22.26	409.2	5345.2	-22.26	0	524.8
	n=50	-	-	8542.6	-	794.1	7825.1	-	-8.40	775.1
	n=100	-	-	11,245.3	-	1674.7	9837.8	-	-12.52	1684.9
T=6	n=5	2468.3	342.6	2468.3	0	98.6	2468.3	0	0	87.5
	n=10	3521.2	1421.3	3521.2	0	154.3	3521.2	0	0	184.2
	n=15	3968.7	3215.8	3968.7	0	202.4	3968.7	0	0	194.6
	n=25	10,482.6	7200[a]	7845.9	-25.15	684.5	7845.9	-25.15	0	708.2
	n=50	-	-	10,813.5	-	948.6	9824.1	-	-9.15	1024.8
	n=100	-	-	14,951.3	-	2074.2	12,909.4	-	-13.66	2042.1

[a] *Premature termination of CPLEX due to limitation of running time.*

4. CASE STUDY

A real-world case is utilised to validate the practical feasibility of the robust TEIRP model and the developed solution algorithm as well as to examine the correlation between optimised outcomes and model inputs. The data in the case are provided by a famous cold chain pharmacy logistics company in Zhejiang, China. *Figure 2* shows the geographical distribution of the study two two-echelon vaccine supply network, containing a vaccine supplier, a distribution warehouse and 20 vaccine demand nodes. The vaccine supplier is not marked in the figure because it is located at another province and far from the distribution warehouse and demand nodes. The nominal value and maximum deviation of vaccine demand at each demand node is collected and estimated from the historical data. The 20-day planning time horizon is divided into four time periods, thus each time period contains five days. Note that each demand node can be served at most once in each period.

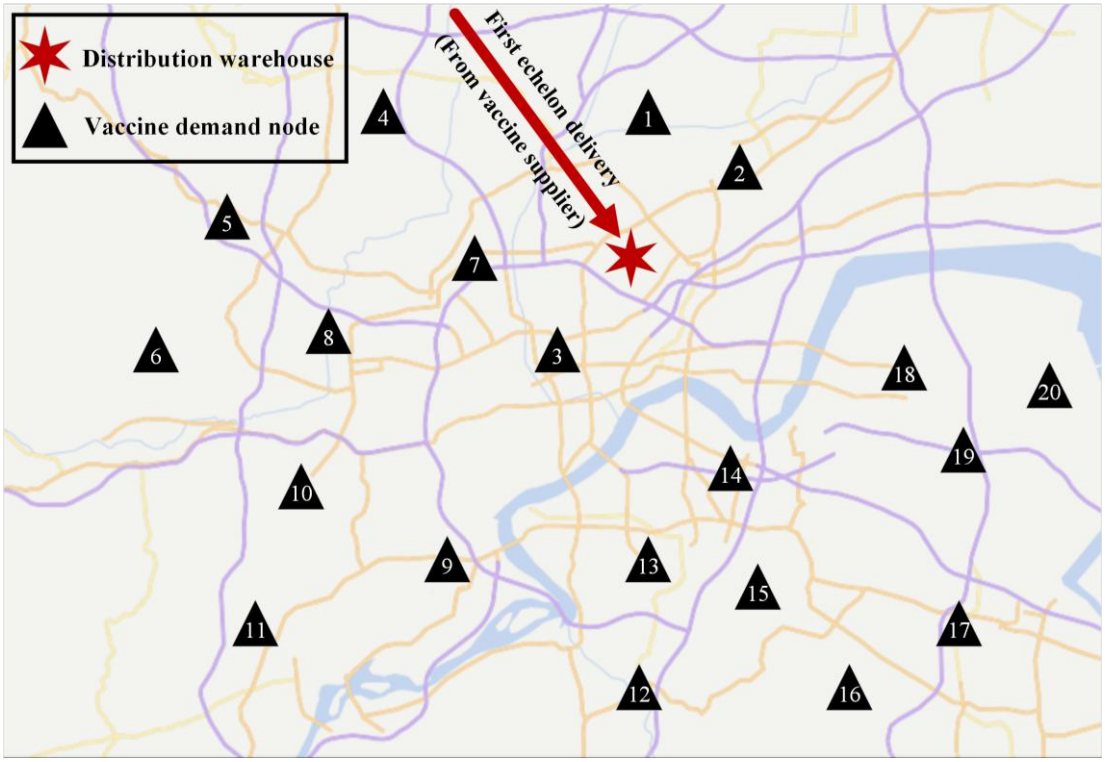

Figure 2 – The study two-echelon vaccine supply network

4.1 Input parameters

Some input parameters that are critical to the optimised results are discussed next. As detailed in *Table 3*, the vehicles employed in the case are classified into two types in accordance with two echelons. The first-echelon vehicle with more capacity is for the line-haul delivery between the supplier and the distribution warehouse. The second-echelon vehicle with less capacity is for the short-haul delivery between the distribution warehouse and demand nodes. *Table 4* illustrates the unit volume of the vaccine types in the case. The degree of conservatism of each demand node is set at 0.5, while the maximum vaccine demand deviation from nominal value of each demand node is defined at 25%. The unit holding cost at the distribution warehouse is set at 3 $yuan/m^3 \cdot day$, whereas the unit holding cost at the demand nodes is set at 5.5 $yuan/m^3 \cdot day$. The unit shortage penalty cost of vaccine is set at 300 $yuan/day$. The initial inventory levels of distribution warehouse and demand node are set at 40% of their inventory holding capacity.

Table 3 – Input parameters of two types of vehicles in different echelons

Vehicle type	Vehicle capacity/m^3	Unit delivery cost/yuan·km^{-1}
First-echelon vehicle	14	7
Second-echelon vehicle	4	3

Table 4 – Input vaccine parameters

Vehicle type	Unit volume/m^3
Vaccine type 1	0.032
Vaccine type 2	0.022
Vaccine type 3	0.018

4.2 Result analysis

In this section, the optimised results of two scenarios (e.g. vaccine shortage is allowed (VSA) or vaccine shortage is not allowed (VSNA)) are compared. As illustrated in the heading rows of *Table 5*, the cost term for the optimised results is decomposed into five cost components, namely the total cost (TC), first-echelon delivery cost (FDC), second-echelon delivery cost (SDC), distribution warehouse inventory cost (DWIC), demand node inventory cost (DNIC) and vaccine shortage penalty cost (PC). The gap between the optimised costs of VSNA and VSA is computed by *Equation 39.*

It can be found that the costs of VSNA scenario are generally higher than that of VSA scenario except the penalty cost. This is because in the shortage-not-allowed scenario, the pharmacy logistics company needs to store and deliver more vaccines to help demand nodes deal with the uncertainty of demand, thus incurring a 103.9% increase of total cost excluding the penalty cost. Note that the DNIC of VSNA is obviously higher than that of VSA. This indicates that in the shortage-not-allowed scenario, the demand nodes (e.g. hospitals, clinics and community healthcare centres) are inclined to maintaining higher vaccine inventory level to deal with the uncertain fluctuations in vaccine demand.

$$\Delta_{GAP} = \frac{Z_{VSNA} - Z_{VSA}}{Z_{VSA}} * 100\% \tag{39}$$

Table 5 – Optimised costs found by deterministic and robust models

Scenarios	TC	DC		IC		PC
		FDC	SDC	DWIC	DNIC	
VSA	739,841.7	123,248.2	265,476.7	96,254.6	24,532.8	230,329.4
VSNA	1,039,025.1	191,354.3	480,157.4	235,718.2	131,795.2	0
Δ_{GAP}	40.44%	55.26%	80.87%	144.89%	437.22%	-

**VSA: vaccine shortage allowed; VSNA: vaccine shortage not allowed; TC: total cost (yuan); DC: total delivery cost (yuan); FDC: first-echelon delivery cost (yuan); SDC: second-echelon delivery cost (yuan); IC: total inventory cost (yuan); DWIC: distribution warehouse inventory cost (yuan); DNIC: demand node inventory cost (yuan); PC: vaccine shortage penalty cost (yuan).*

Tables 6 and *7* detail the delivery schemes of VSNA and VSA respectively, containing the number of vehicles used in 1st echelon and vehicle routes in 2nd echelon. It can be observed that compared to VSA, the delivery scheme of VSNA employs more 1st-echelon and 2nd-echelon vehicles, which is consistent with the results of the optimised costs. Note that 2nd-echelon vehicle in VSNA visited less demand nodes in one service compared to that in VSA, because the demand nodes require more vaccines in VSNA while the capacity of the vehicle is limited. It can also be seen that at the beginning of the planning time horizon (e.g. time period 1), more vehicles are employed both in VSNA and VSA. The reason is that the initial inventory levels of the distribution warehouse and demand nodes are set at only 40%, thus the pharmacy logistics company will assign more vehicles to replenish them in time period 1.

Table 6 – Optimised delivery scheme of VSA

Time period	Number of vehicles used in 1st echelon	Vehicle routes in 2nd echelon
Time period 1	4	0-2-1-4-5-7-0, 0-8-4-10-11-9-0, 0-3-13-12-16-14-0, 0-17-19-20-18-0
Time period 2	2	0-1-4-5-8-3-0, 0-13-12-16-17-19-18-0
Time period 3	3	0-7-10-11-9-12-13-0, 0-3-14-15-16-17-0, 0-18-19-20-2-1-0
Time period 4	3	0-1-4-5-6-8-7-0, 0-10-11-9-13-3-0, 0-14-15-19-18-2-0

Table 7 – Optimised delivery scheme of VSNA

Time period	Number of vehicles used in 1st echelon	Vehicle routes in 2nd echelon
Time period 1	5	0-1-2-7-4-0, 0-5-6-8-10-0, 0-10-11-9-3-0, 0-14-19-20-18-0,0-13-12-16-14-15-0
Time period 2	4	0-3-7-4-1-2-0, 0-9-11-10-8-6-5-0, 0-13-12-16-15-14-0, 0-17-19-20-18-0
Time period 3	4	0-1-4-5-6-0, 0-14-17-19-20-18-2-0, 0-8-11-9-3-0
Time period 4	4	0-1-4-5-6-8-7-0, 0-3-10-11-9-0, 0-13-12-16-17-15-0, 0-14-19-20-18-2-0

4.3 Sensitivity analysis

In this section, the control variates method is used to conduct the sensitivity analysis, further exploring the impacts of the input parameters on the vaccine supply system. Some main parameter values (e.g. the degree of conservatism, maximum vaccine demand deviation, unit vaccine holding cost, unit shortage penalty cost) are varied within their probable ranges. This effort would help decision makers evaluate the performance of the vaccine supply system.

Figure 3 illustrates the influence of the degree of conservatism on the optimised costs, where the degree of conservatism ranges from 0 to 1. A clear trend can be seen that as the degree of conservatism increases from 0 to 0.8, the total cost slightly decreases when the degree of conservatism is less than 0.5 and then drops rapidly to the lowest. As the degree of conservatism continues to increase from 0.8 to 1, the total cost grows back. This trend is caused by the trade-off among delivery cost, inventory cost and penalty cost. It can be seen from the figure that as the degree of conservatism increases from 0.8 to 1, the delivery cost and inventory cost both slightly increase while the penalty cost decreases rapidly. This also indicates that the change in degree of conservatism may affect penalty cost more in the certain range. As the degree of conservatism continues to increase from 0.8 to 1, the delivery cost and inventory cost both keep growing while the downward trend of the penalty cost tends to slow down and converges at 0.

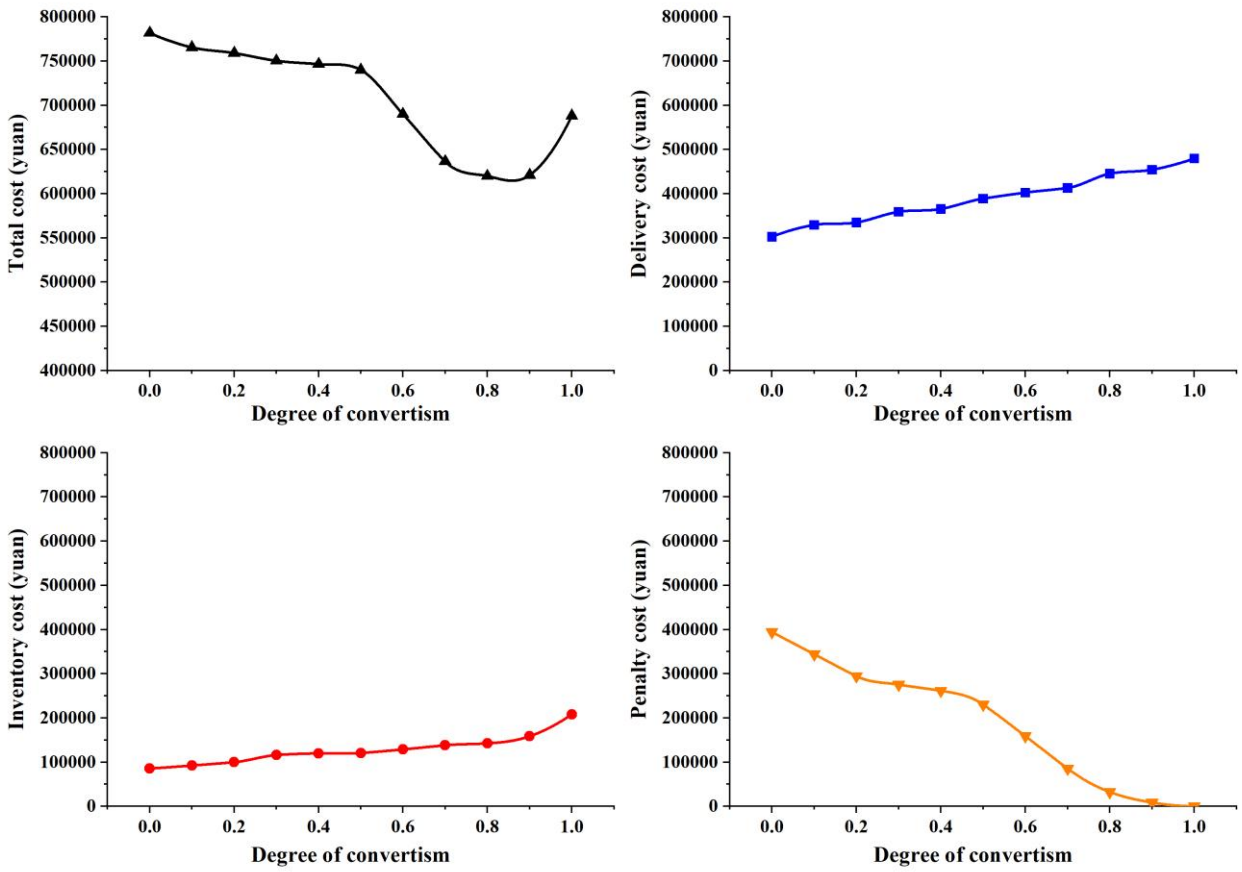

Figure 3 – Optimised costs vs. degree of conservatism

Figure 4 shows the effects of the demand deviation on the optimised costs, where the demand deviation ranges from 0 to 100%. It can be clearly observed from the figure that as the demand deviation increases, the optimised costs (e.g. total cost, delivery cost, inventory cost and penalty cost) all increase. In detail, the delivery cost and inventory cost both slightly increase when demand deviation is less than 80% and then saturate with the increase of the demand deviation. As formulated in *Equations 3*, *5*, *7*, *8*, despite the increasing demand, deviation implies that more vaccines are stored and delivered in each period, the capacities of the vehicles and warehouses are limited. Thus, as the demand deviation keeps increasing from 80% to 100%, delivery and inventory costs tend to converge while the penalty cost grows rapidly.

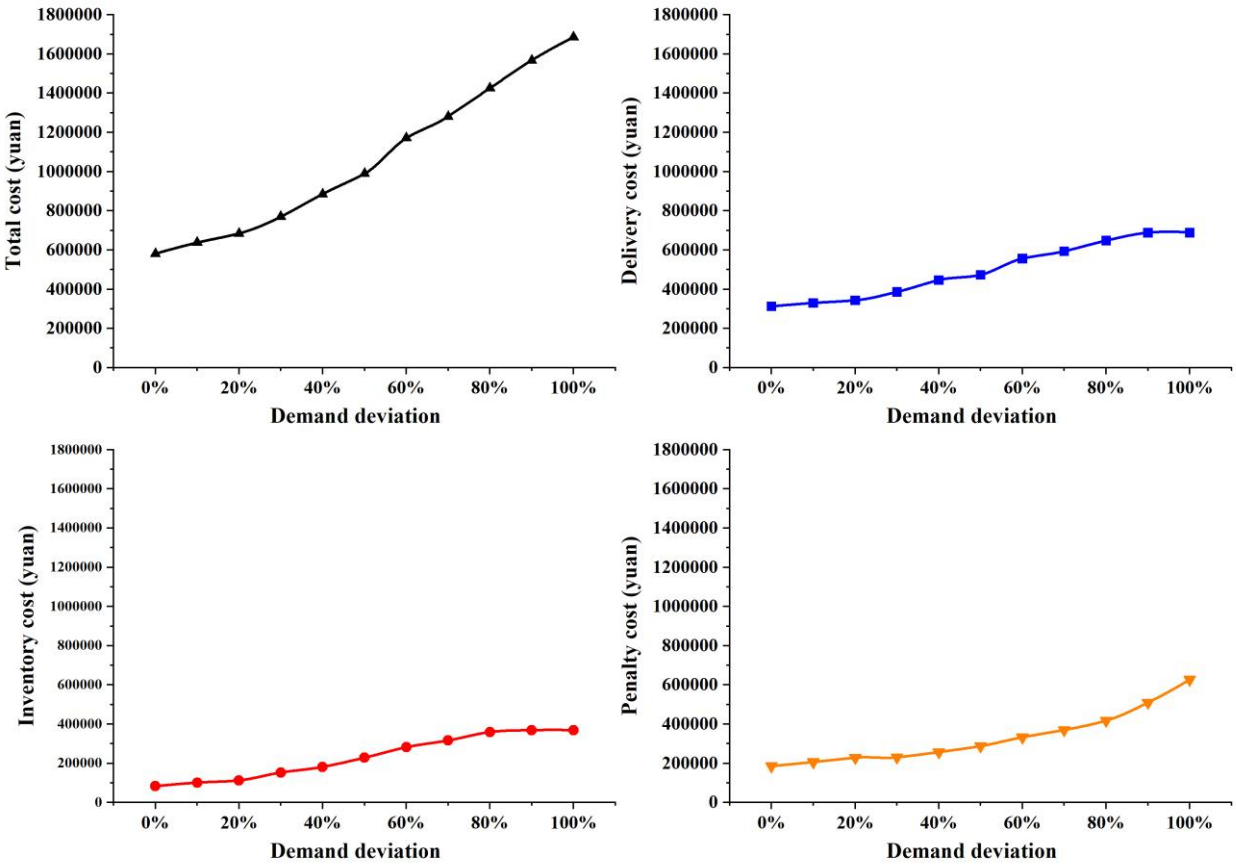

Figure 4 – Optimised costs vs. demand deviation

The effect of the vaccine shortage penalty cost on the optimised costs is analysed in *Figure 5*, where the unit penalty cost ranges from 100 to 600. As can be seen from the figure, with the increase of the unit penalty cost, the inventory cost increases by 453.8% while the delivery cost increases by 87.3%, which indicates that the change in the vaccine shortage penalty cost may affect inventory cost more in the certain range.

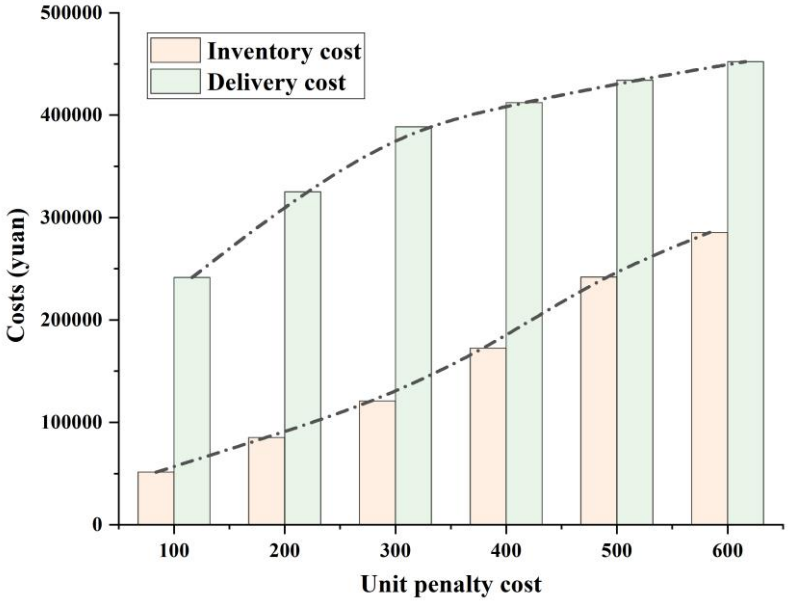

Figure 5 – Optimised costs vs. penalty cost

In *Figure 6*, the influence of the inventory cost of distribution warehouse and demand nodes on the optimised costs are illustrated, where the multiplier varies from 0.5 to 1.5. It can be found that as the unit inventory cost of distribution warehouse increases, the 2nd-echelon delivery cost almost linearly increases while the penalty cost decreases. Opposite trends can be observed when the unit inventory cost of demand nodes increases, which indicates that less vaccines stored in the demand nodes may increase the vaccine shortage penalty cost.

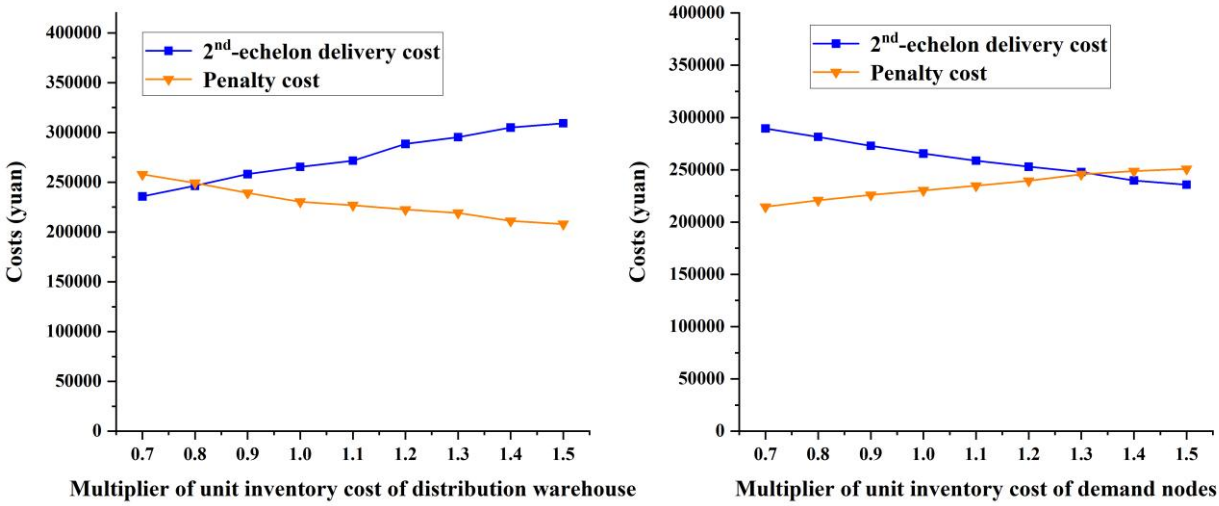

Figure 6 – Optimised costs vs. inventory cost

5. CONCLUSION

This study focuses on the optimisation of a two-echelon vaccine supply system considering uncertain demand. A robust model is formulated to simultaneously optimise the two-echelon vehicle routes as well as inventory at both distribution warehouse and vaccine demand nodes. A tangible heuristic solution algorithm combining SA and ALNS is developed, the computational efficiency of which is verified by numerical experiments in comparison with that of CPLEX and ALNS. A real-world case study is conducted to demonstrate the practical applicability of the proposed model, while the relation among the decision variables and model parameters was explored by the sensitivity analyses. Some major findings include:

1) If the shortage is not allowed in the vaccine supply system, the demand nodes (e.g. hospitals, clinics and community healthcare centres) will be inclined to maintaining higher vaccine inventory level to deal with the uncertain fluctuations in vaccine demand.

2) Higher degree of conservatism will result in more delivery and inventory costs as well as less shortage penalty cost. And if the degree of conservatism increases, the total cost will show an overall trend of first increasing and then decreasing.
3) The increase of vaccine demand deviation will lead to an intense increase of total cost, where delivery and inventory costs both slightly increase in the beginning and then tend to saturate.

The research provides decision makers with an effective methodology to configure the vaccine supply system considering the uncertainty in vaccine demand. However, there are still some limitations in our model. Since there are more uncertain factors (e.g. traffic jam, facilities interruption) in the real-world vaccine supply system, how to take more uncertain parameters into account and develop a model in line with the real-world case may be an important direction for future research. Another immediate extension would be the robust optimisation of two-echelon vaccine supply system containing multiple distribution warehouses.

ACKNOWLEDGEMENTS

This paper was supported by the Zhejiang Provincial Science and Technology Program under grant 2023C01218, Science and Technology Program of Zhejiang Provincial Department of Transport under grant 2024016 and Zhejiang Provincial Statistical Science Research Program under grant 25TJYX01.

REFERENCES

[1] Assiri A, et al. Launching COVID-19 vaccination in Saudi Arabia: Lessons learned, and the way forward. *Travel Medicine and Infectious Disease*. 2021;43:102119. DOI: 10.1016/j.tmaid.2021.102119.

[2] Shen Y, et al. Predicting future vaccination habits: The link between influenza vaccination patterns and future vaccination decisions among old aged adults in China. *Journal of Infection and Public Health*. 2024;17(6):1079-1085. DOI: 10.1016/j.jiph.2024.04.017.

[3] Asundi A, O'leary C, Bhadelia N. Global COVID-19 vaccine inequity: The scope, the impact, and the challenges. *Cell Host & Microbe*. 2021;29(7):1036-1039. DOI: 10.1016/j.chom.2021.06.007.

[4] Castillo JC, et al. Market design to accelerate COVID-19 vaccine supply. *Science*. 2021;371(6534):1107-1109. DOI: 10.1126/science.abg0889.

[5] Georgiadis GP, Georgiadis MC. Optimal planning of the COVID-19 vaccine supply chain. *Vaccine*. 2021;39(37):5302-5312. DOI: 10.1016/j.vaccine.2021.07.068.

[6] Sinha P, Kumar S, Chandra C. Strategies for ensuring required service level for COVID-19 herd immunity in Indian vaccine supply chain. *European Journal of Operational Research*. 2023;304(1):339-352. DOI: 10.1016/j.ejor.2021.03.030.

[7] Geng H, Shi C M. Health policy, price regulation, and innovation: Evidence from China's vaccine industry. *Journal of Development Economics*. 2024;167:103229. DOI: 10.1016/j.jdeveco.2023.103229.

[8] Federgruen A, Zipkin P. A combined vehicle routing and inventory allocation problem. *Operations Research*. 1984;32(5):1019-1037. DOI: 10.1287/opre.32.5.1019.

[9] Jung J, Mathur K. An efficient heuristic algorithm for a two-echelon joint inventory and routing problem. *Transportation Science.* 2007;41(1):55-73. DOI: 10.1287/trsc.1060.0160.

[10] Zhao QH, Chen S, Zang CX. Model and algorithm for inventory/routing decision in a three-echelon logistics system. *European Journal of Operational Research*. 2008;191(3):623-635. DOI: 10.1016/j.ejor.2006.12.056.

[11] Li J, Chu F, Chen H. A solution approach to the inventory routing problem in a three-level distribution system. *European Journal of Operational Research.* 2011;210(3):736-744. DOI: 10.1016/j.ejor.2010.10.020.

[12] Nambirajan R, et al. CARE: Heuristics for two-stage multi-product inventory routing problems with replenishments. *Computers & Industrial Engineering*. 2016;97:41-57. DOI: 10.1016/j.cie.2016.04.004.

[13] Rohmer SUK, Claassen GDH, Laporte G. A two-echelon inventory routing problem for perishable products. *Computers & Operations Research.* 2019;107:156-172. DOI: 10.1016/j.cor.2019.03.015.

[14] Nakhjirkan S, Rafiei FM. An integrated multi-echelon supply chain network design considering stochastic demand: A genetic algorithm based solution. *Promet -Traffic&Transportation*. 2017;29(4):391. DOI: 10.7307/ptt.v29i4.2193.

[15] Guimarães AT, Coelho CL, Schenekemberg MC, Scarpin TC. The two-echelon multi-depot inventory-routing problem. *Computers & Operations Research*. 2019;101:220-233. DOI: 10.1016/j.cor.2018.07.024.

[16] Schenekemberg CM, et al. The two-echelon inventory-routing problem with fleet management. *Computers & Operations Research*. 2020;121:104944. DOI: 10.1016/j.cor.2020.104944.

[17] Farias K, Hadj-Hamou K, Yugma C. Model and exact solution for a two-echelon inventory routing problem. *International Journal of Production Research*. 2021;59(10):3109-3132. DOI: 10.1080/00207543.2020.1746428.

[18] Charaf S, Taş D, Flapper SDP, Woensel V. A branch-and-price algorithm for the two-echelon inventory-routing problem. *Computers & Industrial Engineering*. 2024;196:110463. DOI: 10.1016/j.cie.2024.110463.

[19] Charaf S, Taş D, Flapper SDP, Woensel V. A matheuristic for the two-echelon inventory-routing problem. *Computers & Operations Research*. 2024;171:106778. DOI: 10.1016/j.cor.2024.106778.

[20] Soyster AL. Technical note—Convex programming with set-inclusive constraints and applications to inexact linear programming. *Operations Research*. 1973;21(5):1154-1157. DOI: 10.1287/opre.21.5.1154.

[21] Bertsimas D, Sim M. Robust discrete optimization and network flows. *Mathematical Programming*. 2003;98(1):49-71. DOI: 10.1007/s10107-003-0396-4.

[22] Bertsimas D, Sim M. The price of robustness. *Operations Research*. 2004;52(1):35-53. DOI: 10.1287/opre.1030.0065.

[23] Huang SH, Lin PC. A modified ant colony optimization algorithm for multi-item inventory routing problems with demand uncertainty. *Transportation Research Part E: Logistics and Transportation Review*. 2010;46(5):598-611. DOI: 10.1016/j.tre.2010.01.006.

[24] Solyalı O, Cordeau JF, Laporte G. Robust inventory routing under demand uncertainty. *Transportation Science*. 2012;46(3):327-340. DOI: 10.1287/trsc.1110.0387.

[25] Soysal M, Bloemhof-Ruwaard JM, Haijema R, van der Vorst JGA. Modelling an inventory routing problem for perishable products with environmental considerations and demand uncertainty. *International Journal of Production Economics*. 2015;164:118-133. DOI: 10.1016/j.ijpe.2015.03.008.

[26] Li M, Wang Z, Chan FTS. A robust inventory routing policy under inventory inaccuracy and replenishment lead-time. *Transportation Research Part E: Logistics and Transportation Review*. 2016;91:290-305. DOI: 10.1016/j.tre.2016.05.001.

[27] Jafarkhan F, Yaghoubi S. An efficient solution method for the flexible and robust inventory-routing of red blood cells. *Computers & Industrial Engineering*. 2018;117:191-206. DOI: 10.1016/j.cie.2018.01.029.

[28] Fardi K, Jafarzadeh GS, Hafezalkotob A. An extended robust approach for a cooperative inventory routing problem. *Expert Systems with Applications*. 2019;116:310-327. DOI: 10.1016/j.eswa.2018.09.002.

[29] Rodrigues F, et al. Comparing techniques for modelling uncertainty in a maritime inventory routing problem. *European Journal of Operational Research*. 2019;277(3):831-845. DOI: 10.1016/j.ejor.2019.03.015.

[30] Liu B, Zhang Q, Yuan Z. Two-stage distributionally robust optimization for maritime inventory routing. *Computers & Chemical Engineering*. 2021;149:107307. DOI: 10.1016/j.compchemeng.2021.107307.

[31] Taghipour A, et al. A robust vaccine supply chain model in pandemics: Case of Covid-19 in Iran. *Computers & Industrial Engineering*. 2023;183:109465. DOI: 10.1016/j.cie.2023.109465.

[32] Li R, Cui Z, Kuo YH, Zhang L. Scenario-based distributionally robust optimization for the stochastic inventory routing problem. *Transportation Research Part E: Logistics and Transportation Review*. 2023;176:103193. DOI: 10.1016/j.tre.2023.103193.

[33] Ortega EJA, et al. Stochastic inventory routing with dynamic demands and intra-day depletion. *Computers & Operations Research*. 2024;163:106503. DOI: 10.1016/j.cor.2023.106503.

[34] Ji Y, et al. A mixed integer robust programming model for two-echelon inventory routing problem of perishable products. *Physica A: Statistical Mechanics and its Applications*. 2020;548:124481. DOI: 10.1016/j.physa.2020.124481.

[35] Shang X, Zhang G, Jia B, Almanaseer M. The healthcare supply location-inventory-routing problem: A robust approach. *Transportation Research Part E: Logistics and Transportation Review*. 2022;158:102588. DOI: 10.1016/j.tre.2021.102588.

[36] Rave A, Fontaine P, Kuhn H. Cyclic stochastic two-echelon inventory routing for an application in medical supply. *European Journal of Operational Research*. 2025;325(1):81-99. DOI: 10.1016/j.ejor.2025.02.032.

[37] Shiri M, Fattahi P, Sogandi F. Two-stage approach for COVID-19 vaccine supply chain network under uncertainty using the machine learning algorithms: A case study. *Engineering Applications of Artificial Intelligence.* 2024;135:108837. DOI: 10.1016/j.engappai.2024.108837.

[38] Archetti C, Bertazzi L, Laporte G, Speranza,MG. A branch-and-cut algorithm for a vendor-managed inventory-routing problem. *Transportation Science*. 2007;41(3):382-391. DOI: 10.1287/trsc.1060.0188.

[39] Pisinger D, Ropke S. A general heuristic for vehicle routing problems. *Computers & Operations Research*. 2007;34(8):2403-2435. DOI: 10.1016/j.cor.2005.09.012.

[40] Ghilas V, Demir E, Van Woensel T. An adaptive large neighbourhood search heuristic for the pickup and delivery problem with time windows and scheduled lines. *Computers & Operations Research*. 2016;72:12-30. DOI: 10.1016/j.cor.2016.01.018.

[41] Liu R, Tao Y, Xie X. An adaptive large neighbourhood search heuristic for the vehicle routing problem with time windows and synchronized visits. *Computers & Operations Research*. 2019;101:250-262. DOI: 10.1016/j.cor.2018.08.002.

[42] Gao T, et al. Optimising electric flex-route feeder transit service with dynamic wireless charging technology. *Promet - Traffic&Transportation*. 2024;36(4):654-672. DOI: 10.7307/ptt.v36i4.494.

[43] Coelho LC, Cordeau JF, Laporte G. The inventory-routing problem with transshipment. *Computers & Operations Research*. 2012;39(11):2537-2548. DOI: 10.1016/j.cor.2011.12.020.

[44] Ma B, et al. Time-dependent vehicle routing problem with departure time and speed optimization for shared autonomous electric vehicle service. *Applied Mathematical Modelling*. 2023;113:333-357. DOI: 10.1016/j.apm.2022.09.020.